Acta Crystallographica Section D
Biological Crystallography
ISSN 0907-4449

Crystallization and preliminary X-ray characterization of cytochrome *c*″ from the obligate methylotroph *Methylophilus methylotrophus*

Francisco J. Enguita,[a] Luisa Rodrigues,[a] Margarida Archer,[a] Larry Sieker,[b] Artur Rodrigues,[a] Ehmke Pohl,[c] David L. Turner,[d] Helena Santos[a] and Maria Arménia Carrondo[a]*

[a]Instituto de Tecnologia Química e Biológica, Universidade Nova de Lisboa, 2781-901 Oeiras, Portugal, [b]Department of Biological Structure, Box 357420, University of Washington, Seattle WA 98195, USA, [c]EMBL Hamburg Outstation, Norkestrasse 85, 22603 Hamburg, Germany, and [d]Department of Chemistry, University of Southampton, Southampton, England

Correspondence e-mail: carrondo@itqb.unl.pt

Received 3 September 2002
Accepted 10 January 2003

Cytochrome *c*″ from the obligate methylotroph *Methylophilus methylotrophus* is a 15 kDa monohaem protein which has a *c*-type haem covalently linked to the protein chain. Two histidine residues are the axial ligands of the Fe atom in the oxidized form. This cytochrome is one of the few known haem proteins which undergoes a change of spin state of the Fe atom upon reduction, with the detachment of an axial histidine ligand. Initial crystallization conditions involved the utilization of cadmium chloride as an additive and resulted in highly mosaic crystals with poor diffraction properties. Optimization of the crystallization conditions was achieved by slowing the nucleation process utilizing agarose gels and viscous additives such as PEG, ethylene glycol and glycerol. Addition of glycerol to the crystallization buffer produced crystals suitable for X-ray diffraction, with a reduced solvent content and mosaicity, which diffracted to a maximum resolution of 1.19 Å using synchrotron radiation. The crystals obtained under these conditions were employed for structure solution using the multiwavelength anomalous dispersion method at the Fe *K* edge.

1. Introduction

Cytochrome *c*″ is a monohaem protein isolated from the obligate methylotroph *Methylophilus methylotrophus*. It comprises 124 amino acids in the final processed form, with a haem *c* group covalently linked to the protein chain by the consensus sequence C*XX*CH. In the oxidized form, the axial coordination of the Fe atom within the haem group is made by a pair of histidines, with an almost perpendicular orientation of the imidazole-ring planes (Berry *et al.*, 1990).

The cytochrome *c*″ sequence has two unusual features: firstly, the location of the haem-binding cysteines is far downstream from the N-terminus, namely at positions 49 and 52, and, secondly, an extra pair of cysteine residues is present near the C-terminus and forms a disulfide bridge (Brennan *et al.*, 2001). In both respects, cytochrome *c*″ is similar to the oxygen-binding haem protein SHP from the purple phototrophic bacterium *Rhodobacter sphaeroides* (Klarskov *et al.*, 1999). SHP exhibits detachment of one of the haem axial ligands, an asparagine, upon reduction. Cytochrome *c*″ also changes from low-spin to high-spin upon reduction owing to the dissociation of a sixth haem ligand, which was identified as His95 by analogy to the class I cytochromes *c* (Costa *et al.*, 1992*a*). The sequence positions of haem-binding cysteines and the presence of certain consensus residues suggests that cytochrome *c*″ is the second example of a variant class I cytochrome *c* (Klarskov *et al.*, 1998). The midpoint redox potential of cytochrome *c*″ (−60 mV at pH 7.0) shows a strong pH dependence in the physiological range, for which the ionization of the detached histidine in the reduced form is mainly responsible (Costa *et al.*, 1992*b*). Cytochrome *c*″ is a unique example of a haem *c* protein with bis-histidine coordination and spectroscopic properties similar to those observed in model compounds where axial ligand planes are forced into perpendicular orientations by steric constraints (Safo *et al.*, 1991).

The physiological function of cytochrome *c*″ remains unknown; however, the characteristic arrangement of the axial haem ligands and the changes occurring in this coordination upon reduction make cytochrome *c*″ an interesting example of a redox protein, providing a simple model for the understanding of redox reactions in more complex systems.

2. Materials, methods and results

2.1. Protein crystallization

The oxidized form of native cytochrome *c*″ from *M. methylotrophus* was purified as described previously (Costa *et al.*, 1992*b*). Crystallization trials were set up by either vapour-diffusion or microbatch techniques at 298 K. After several months, a single crystal

Table 1
Characteristics of cytochrome *c*′′ crystals obtained under different conditions during the optimization process.

	Crystals in Fig. 1(*a*)	Crystals in Fig. 1(*b*)	Crystals in Fig. 1(*c*)
Crystallization technique	Vapour diffusion (sitting drop)	Diffusion into capillaries	Vapour diffusion (sitting drop)
Crystallization conditions	2.5 *M* $(NH_4)_2SO_4$, 0.1 *M* Tris–maleate buffer pH 7.0, 5 m*M* $CdCl_2$	3.5 *M* $(NH_4)_2SO_4$, 0.1 *M* Tris–maleate buffer pH 7.0, 5 m*M* $CdCl_2$, 0.2% agarose	2.5 *M* $(NH_4)_2SO_4$, 20% glycerol, 0.1 *M* Tris–maleate buffer pH 7.0, 2.5 m*M* $CdCl_2$
Maximum dimensions (µm)	300 × 300 × 800	150 × 200 × 500	150 × 150 × 400
Place of data collection	Beamline ID-14-2, ESRF, Grenoble, France	In-house rotating anode	Beamline X-11, EMBL, Hamburg, Germany
Data-collection temperature (K)	110	293	110
Space group	$P2_12_12_1$	$P2_12_12_1$	$P2_12_12_1$
Unit-cell parameters (Å, °)	a = 81.28, b = 161.71, c = 344.52, $\alpha = \beta = \gamma = 90$	a = 81.56, b = 165.12, c = 330.66, $\alpha = \beta = \gamma = 90$	a = 58.53, b = 74.11, c = 78.38, $\alpha = \beta = \gamma = 90$
Molecules in the asymmetric unit	16	16	2
Mosaicity	1.20	0.90	0.45
Approx. solvent content (%)	75	63	51
Diffraction limits	25.0–5.50	25.0–3.50	25.0–1.19

Table 2
Data-collection statistics of cytochrome *c*′′ crystals.

Values in parentheses are for the outer resolution shell.

	High resolution	Fe peak	Fe inflection	Fe remote
Place of data collection	EMBL, Hamburg, Germany	EMBL, Hamburg, Germany		
Beamline	X11	BW7A		
Wavelength (Å)/Energy (eV)	0.933	1.7400/7125.5	1.7450/7105.1	1.2397/10001.2
Space group	$P2_12_12_1$			
Unit-cell parameters (Å, °)	a = 58.4, b = 74.2, c = 77.9, $\alpha = \beta = \gamma = 90.0$	a = 58.3, b = 74.2, c = 77.8, $\alpha = \beta = \gamma = 90.0$		
Resolution limits (Å)	25.0–1.19 (1.22–1.19)	25.0–2.00 (2.05–2.00)	25.0–2.00 (2.05–2.00)	25.0–1.80 (1.84–1.80)
Total No. of reflections	451489	223949	225242	486259
No. of unique reflections	102739	23423	23422	32089
Average redundancy	4.31	8.90	8.77	14.05
Completeness (%)	100.0	100.0	99.9	99.9
$I/\sigma(I)$	6.10 (2.05)	14.75 (6.25)	12.55 (3.74)	12.35 (3.75)
R_{merge}† (%)	5.1 (38.4)	7.9 (18.4)	8.1 (25.5)	8.5 (23.3)
$R_{r.i.m.}$‡ (%)	5.8 (37.8)	7.1 (16.2)	7.2 (23.3)	6.3 (19.7)
$R_{p.i.m.}$‡ (%)	2.7 (18.0)	2.3 (5.4)	2.4 (7.8)	1.7 (5.2)
R_{anom}§ (%)	—	5.4	4.4	2.9

† $R_{merge} = \sum_{hkl}\sum_i |I_i(hkl) - \overline{I(hkl)}|/\sum_{hkl}\sum_i I_i(hkl)$. ‡ Defined in Weiss (2001). § $R_{anom} = \sum |I^+ - I^-|/\sum |I^+ + I^-|$, where I^+ and I^- denote the mean intensity values of each mate in a Bijvoet pair.

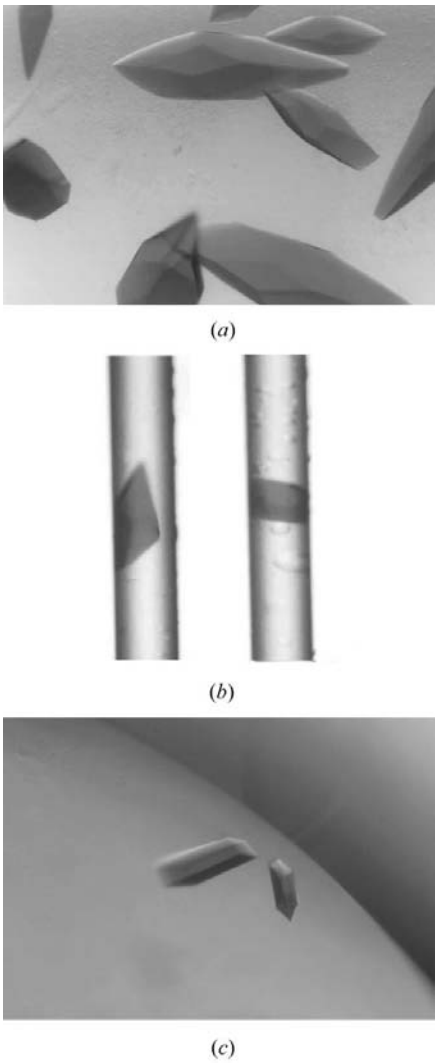

Figure 1
Photographs of cytochrome *c*′′ crystals obtained using different crystallization conditions and methods (see Table 1). From (*a*) to (*c*) a decrease in crystal mosaicity and solvent content was observed. (*a*) Crystals obtained using the initial conditions by vapour diffusion, (*b*) crystals obtained by diffusion into capillaries with the protein gelled with 0.2% agarose and (*c*) optimized crystals obtained by vapour diffusion in the presence of 20% glycerol, used for structure solution and high-resolution data collection.

was found in one sitting drop containing 30 mg ml^{-1} native protein, 1.8 *M* ammonium sulfate, 0.1 *M* Tris–HCl pH 7.0 and 5 m*M* cadmium chloride. Cadmium chloride was also added to several droplets that remained clear during this period of time and crystals appeared in the droplets containing ammonium sulfate as precipitant within several days. However, crystals grown under these conditions were not useful for X-ray diffraction experiments (see Table 1 for details).

Further optimization of crystal growth was performed using the method described by López-Jaramillo *et al.* (2001) with minor modifications. 18 mg ml^{-1} protein solution buffered with 100 m*M* Tris–maleate pH 7 was gelled with 0.2% agarose at 313 K and the resulting solution used to fill a capillary tube (0.3 mm width × 60 mm length). Precipitant solution containing 2–3 *M* ammonium sulfate and 5–10 m*M* $CdCl_2$ was poured into the top of the capillary tube and the system was sealed with vacuum grease and stored at 295 K for crystal growth. Under these conditions, crystal growth typically took 20–60 d depending on the precipitant concentration (Fig. 1).

Crystal growth in the capillaries was slower than in the vapour-diffusion method and also resulted in an increased crystal quality for X-ray diffraction studies (Table1).

For slowing the process in the sitting-drop system, several viscous additives such as glycerol, PEG and ethylene glycol were added to the drops at different concentrations. Crystals were only obtained with glycerol in the concentration range 5–20%. Increasing the concentration of glycerol changed the external shape of the crystals (see Fig. 1) and also improved their X-ray diffraction quality. Optimal conditions for growing X-ray quality crystals in a sitting-drop vapour-diffusion system were a protein concentration of 20 mg ml^{-1} and a reservoir solution consisting of 100 m*M* Tris–maleate buffer pH 7, 20% glycerol, 2.55 *M* ammonium sulfate and 2.5 m*M* $CdCl_2$. Under these conditions, crystals appeared within three to four weeks and reached maximum dimensions of 150 × 150 × 400 µm. Optimized cytochrome *c*′′ crystals belong to space group $P2_12_12_1$, with unit-cell parameters a = 58.4, b = 74.1, c = 78.0 Å, a unit-cell volume of 3.38 × 10^6 Å^3 and two protein molecules per asymmetric unit (Fig. 1).

2.2. X-ray measurements and data processing

High-resolution X-ray diffraction data were collected to a resolution limit of 1.19 Å at the EMBL Hamburg Outstation, Germany (beamline X11), using a MAR-165 CCD detector. X-ray data were processed with *MOSFLM* (Leslie, 1992) and scaled with *SCALA* (Collaborative Computational Project, Number 4, 1994). Details of data processing and statistics are given in Table 2. The Matthews coefficient (Matthews, 1968) for cytochrome *c*′′ crystals was calculated on the basis of two 15 kDa molecules per asymmetric unit, giving a value of 2.8 $Å^3$ Da^{-1}, corresponding to an estimated solvent content of 51%.

Initial attempts to solve the structure of cytochrome *c*′′ used molecular replacement with the average of 20 NMR solutions, as previously determined by Brennan *et al.* (2001), as an initial model. Molecular-replacement solutions found by *MOLREP* (Vagin & Teplyakov, 1997) showed a correlation coefficient of 0.42 and a *R* factor of 0.51 for the first molecule in the asymmetric unit and a correlation coefficient of 0.49 and an *R* factor of 0.43 for the second molecule. Unfortunately, the resulting electron-density maps were poorly defined in the external regions of the protein. However, because cytochrome *c*′′ crystals contained Fe, we decided to use this atom as an anomalous scatterer for structure determination using the multiwavelength anomalous dispersion (MAD) method. For this purpose, a MAD experiment at the iron edge was performed at EMBL, Hamburg, Germany. X-ray data were collected at EMBL beamline BW7A using a MAR165 CCD detector. Based on the X-ray absorption spectrum of cytochrome *c*′′ crystals, two energies were chosen near the *K* absorption edge of the Fe atom: 7.125 keV (λ = 1.7400 Å, peak) and 7.105 keV (λ = 1.7450 Å, point of inflection). The third energy was selected at 10.00 keV (λ = 1.2397 Å) as a high-energy remote point. The crystal diffracted to a maximum resolution of 1.80 Å at the high-energy remote wavelength. The three data sets corresponding to the MAD experiment were processed with *MOSFLM* (Leslie, 1992) and scaled individually with *SCALA* (Collaborative Computational Project, Number 4, 1994).

2.3. Structure determination by the MAD method

For structure solution the MAD method was used (see Table 2 for data-collection statistics). Peak, point of inflection and high-energy remote data sets were scaled together with *SCALEIT* from the *CCP*4 suite (Howell & Smith, 1992). *SOLVE* v.2.02 (Terwilliger & Berendzen, 1999) was used for interpretation of anomalous Patterson maps (Fig. 2), localization of the Fe atoms within the protein structure, refinement of their positional parameters and phasing. The best solution of automated Patterson interpretation clearly determined the position of two of the Fe atoms expected in the asymmetric unit, with a mean figure of merit of 0.69 and an overall *Z* score of 8.7. *SOLVE* was also able to locate one of the S atoms belonging to a cysteine covalently linked to the haem group. Refined positional parameters for these two Fe atoms were used to calculate initial phases and electron-density maps, which showed a clear distinction between protein and solvent regions, indicating that the Patterson solution was correct (Fig. 2). The initial phases (Fig. 2*a*) were further improved by density modification (Fig. 2*b*) with *RESOLVE* (Terwilliger, 2001), with a calculated final figure of merit of 0.75.

3. Discussion

Crystallization of cytochrome *c*′′ was a very difficult and time-consuming task. Over several years, various proteins batches, either native or recombinantly expressed, were submitted to crystallization screenings under different conditions. Preliminary observations indicated that the use of ammonium sulfate as a precipitating agent produced microcrystalline precipitates of the protein. However, a drop containing ammonium sulfate as precipitant and cadmium chloride as an additive showed the presence of one single crystal, revealing that the 'magic bullet' for cytochrome *c*′′ crystallization was cadmium chloride (neither zinc nor calcium worked), which was useful in the concentration range 1–10 m*M*. Unfortunately, crystals obtained under these conditions had a very high solvent content (approximately 75%) and an elevated mosaicity, denoting low internal order of the crystal lattice. As a direct consequence, their diffraction power was very low, reaching a diffraction limit of 5.5 Å at the ID14-2 beamline, ESRF, Grenoble. Crystal growth using 2.5 *M* ammonium sulfate and 10 m*M* $CdCl_2$ was very fast (typically taking 12–36 h to reach crystal dimensions of 300 × 300 × 800 µm) and could be responsible for the lack of internal order of the crystals. In order to slow the crystal-growth process and reduce the convection in the protein solutions, two main strategies were followed: crystallization inside capillaries with agarose-gelled protein solution and addition of viscous additives to the crystallization buffer. Both of these resulted in increased crystal order and decreased solvent content

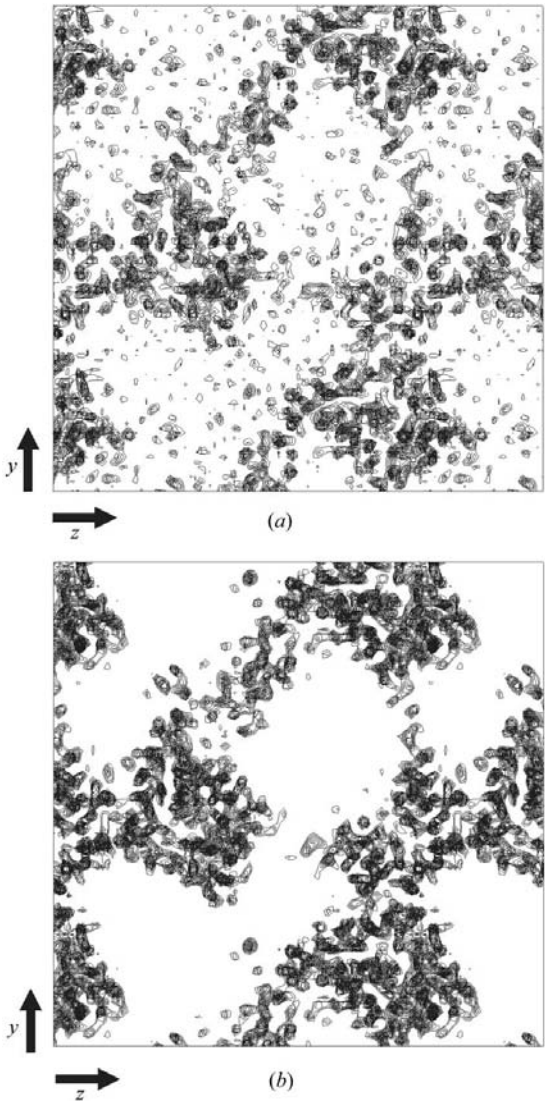

Figure 2
Superposition of 12 electron-density map sections from a total of 95 calculated using the initial MAD phases (*a*) and density-modified with *RESOLVE* (Terwilliger, 2001) (*b*) to a resolution of 2.5 Å. Contours were drawn at 0.5 unit intervals, starting from 1.5. Plots were prepared with *NPO* and *XPLOT84_DRIVER* from the *CCP*4 suite (Collaborative Computational Project, Number 4, 1994).

and mosaicity, improving the X-ray diffraction properties of the resulting crystals. In the case of viscous additives, the use of glycerol in the concentration range 10–25%(*v*/*v*) notably improved the diffraction limits of the cytochrome *c*″ crystals.

Once crystals suitable for X-ray diffraction experiments had been obtained, the initial strategy for cytochrome *c*″ structure solution was molecular replacement using the available NMR structure of the same protein as an initial model (Brennan *et al.*, 2001). However, the intrinsic nature of the NMR models conditioned the resulting phases, producing very well defined electron-density maps in the core haem-binding region of the protein but very sparse electron density in the external protein surface. Electron-density maps obtained with molecular-replacement phases allowed only 50% of the protein chain to be located, making the chain-tracing process very difficult. For this reason, we decided to perform a MAD experiment at the Fe *K* edge in order to improve the experimental phases.

After collecting a complete MAD data set, analysis of Bijvoet and dispersive Patterson maps clearly showed the presence of an anomalous scatterer signal (data not shown). The strongest peaks in Harker sections arose from cross vectors between the two Fe atoms within the asymmetric unit. Automated interpretation of the anomalous difference Patterson map using *SOLVE* (Terwilliger & Berendzen, 1999) determined the coordinates of these Fe atoms within the structure. After refinement of heavy-atom positional parameters and initial phase calculation and despite the poor phasing statistics, the calculated maps unambiguously showed the molecular boundary within the asymmetric unit after map improvement and solvent flipping (Fig. 2*b*). Phase extension of the initial phases to 1.19 Å with *DM* (Cowtan, 1994) using the maximum-resolution data set available allowed the haem group and its ligands to be visualized clearly inside a pocket mainly constituted of α-helices. Model building and structure refinement are presently under way.

Access to the EMBL Hamburg Facility was supported by the European Commission 'Access to Research Infrastructure Action of the Improving Human Potential Programme' (Contract No. HPRI-1999-CT-00017). The ESRF at Grenoble, France is thanked for the provision of data-collection facilities on beamline ID14-EH2. FJE was supported by an EMBO long-term fellowship followed by a PRAXIS XXI post-doctoral fellowship (FCT, Ministério de Ciência e Tecnologia, Portugal). MLR and MA were also supported by PRAXIS XXI fellowships.

References

Berry, M. J., George, S. J., Thompson, A. J., Santos, H. & Turner, D. L. (1990). *Biochem. J.* **270**, 413–417.
Brennan, L., Turner, D. L., Faraleira, P. & Santos, H. (2001). *J. Mol. Biol.* **308**, 353–365.
Collaborative Computational Project, Number 4 (1994). *Acta Cryst.* D**50**, 760–763.
Costa, H. S., Santos, H., Turner, D. L. & Xavier, A. V. (1992*a*). *Eur. Biophys. J.* **25**, 19–24.
Costa, H. S., Santos, H., Turner, D. L. & Xavier, A. V. (1992*b*). *Eur. J. Biochem.* **208**, 427–433.
Cowtan, K. (1994). *Jnt CCP4/ESF–EACBM Newsl. Protein Crystallogr.* **31**, 34–38.
Howell, P. L. & Smith, G. D. (1992). *J. Appl. Cryst.* **25**, 81–86.
Klarskov, K., Leys, D., Backers, K., Costa, H. S., Santos, H., Guisez, H. & Van Beeumen, J. J. (1999). *Biochim. Biophys. Acta*, **1412**, 47–55.
Klarskov, K., Van Driessche, G., Backers, K., Dumortier, C., Meyer, T. E., Tollin, G., Cusanovich, M. A. & Van Beeumen, J. J. (1998). *Biochemistry*, **37**, 5995–6002.
Leslie, A. G. W. (1992). *Crystallographic Computing 5. From Chemistry to Biology*, edited by D. Moras, A. D. Podjarny & J. C. Thierry. Oxford University Press.
López-Jaramillo, J., Garcia-Ruiz, J. M., Gavira, J. A. & Otalora, F. (2001). *J. Appl. Cryst.* **34**, 365–370.
Matthews, B. W. (1968). *J. Mol. Biol.* **33**, 491–497.
Safo, M. K., Gupta, G. P., Walker, F. A. & Scheidt, W. R. (1991). *J. Am. Chem. Soc.* **113**, 5497–5510.
Terwilliger, T. C. (2001). *Acta Cryst.* D**57**, 1755–1762.
Terwilliger, T. C. & Berendzen, J. (1999). *Acta Cryst.* D**55**, 849–861.
Vagin, A. & Teplyakov, A. (1997). *J. Appl. Cryst.* **30**, 1022–1025.
Weiss, M. S. (2001). *J. Appl. Cryst.* **34**, 130–135.